

Peak Shaving Mechanism Employing a Battery Storage System (BSS) and Solar Forecasting

Lau Chee Yong[†], Non-member

ABSTRACT

Maximum demand (kW) has contributed significantly to expensive electricity bills. A modern-day solution for overcoming the penalty demand charges is to utilize the peak shaving method. To perform peak shaving, a battery storage system (BSS) is used. This method involves the charging and discharging of the battery during high and low demand respectively, thus reducing the penalty incurred from the electricity utility company. To charge the battery, a photovoltaic (PV) system is coupled with the BSS. There is currently no BSS algorithm in existence under the microgrid to shave maximum demand with the aid of solar forecasting. In this paper, an algorithm for the BSS to achieve peak shave will be developed with the use of solar PV forecasting. The load profile of a building is used in this study as a reference for future consumption. The developed algorithm releases the energy stored in the BSS to shave the critical demand based on solar forecasting and the BSS state of charge (SOC). In short, this algorithm provides a green solution for reducing the demand charges from the electricity company.

Keywords: Battery storage system, Energy management system, Peak shaving

1. INTRODUCTION

In Malaysia, electricity bills are normally made up of two charges for industrial and commercial buildings, namely consumption and demand. The consumption charge (kWh) is the amount of electricity consumed over a certain period, while the demand charge (kW) is the rate at which the electricity is consumed. Demand charges usually apply to large energy consumers (medium and high voltage levels). Electricity companies can penalize consumers for high electricity demand since it forces them to take further action to ensure sufficient electricity generation, transmission, and distribution capacity to meet demand [1].

Three options are proposed for peak shaving. Firstly, the integration of BSS. During off-peak periods, the system charges the BSS from a source and discharges

Manuscript received on June 17, 2022; revised on August 2, 2022; accepted on August 10, 2022. This paper was recommended by Associate Editor Kaan Kerdchuen.

[†]Corresponding author: laucheeyong@staffemail.apu.edu.my

©2023 Author(s). This work is licensed under a Creative Commons Attribution-NonCommercial-NoDerivs 4.0 License. To view a copy of this license visit: <https://creativecommons.org/licenses/by-nc-nd/4.0/>.

Digital Object Identifier: 10.37936/ecti-eec.2023212.249826

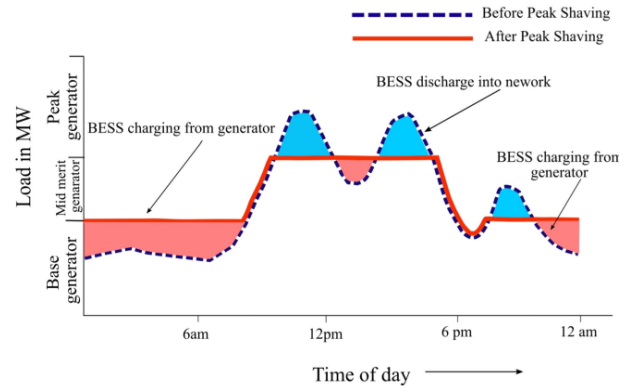


Fig. 1: Peak Shaving using BSS [6].

when demand is high. For a middle-scale system, BSS is the most promising peak shaving process. The downside of this method is the computational load for scheduling and size of the BSS required to achieve optimum operation. Secondly, the integration of electric vehicles (EV) with the grid [2]. This method uses the unutilized battery of the EV to shave the peaks, although the lack of EVs is the main challenge. EVs only supply power while parked. Finally, demand side management (DSM) [3]. This applies to initiatives that may affect consumers in balancing their electricity demand with the generation capability of the power supply system. The main disadvantage of this approach is the complexity of the overall system and lack of ICT infrastructure [4, 5].

Fig. 1 shows how peak shaving can stabilize power consumption. Utilizing BSS to shave peak load benefits both the grid operator and end-user while also reducing carbon emission. Grid operators will be able to solve the ongoing issue of power quality by preventing instability, a sudden blackout, or voltage fluctuations. End-users get to reduce their electricity bill and receive good power quality. Peak shaving with BSS can reduce carbon emissions, helping power plants to operate more efficiently and minimizing load variability [4, 7].

In recent years, battery technology improved significantly in terms of cost and energy density. With the recent advancements, the cost to construct a BSS has decreased exponentially, leading to an improvement in economic viability and net present value (NPV). This in turn will lead to higher demand for the BSS in the future to solve many modern-day electrical power issues [8, 9].

The modern BSS uses Li-ion batteries due to its energy density being suitable for operating at distribution transformer level, lightweight properties, and high efficiency

(roughly 80%). The Hornsdale Power Reserve is the world's largest lithium battery system (100 MW) to date, located in South Australia. This battery farm started operating in November 2017 and was revealed to have a beneficial impact on the local grid.

However, many power consumers are still unaware of the economic feasibility and potential of installing a BSS to reduce their electricity bills. The ROI based on the cost and operation of the system to the profit remains uncertain for these consumers.

With the aim of helping to reduce costly maximum demand charges from electricity companies, a peak shaving algorithm which uses BSS and solar forecasting is proposed and developed in this study. The price of the battery setup, operation cost, and the potential revenue generated are analyzed, along with the capacity of the BSS and charging and discharging time of the battery system. A method for determining and analyzing these parameters was formulated by [10]. The algorithm developed must be able to release the energy stored to shave the critical maximum demand and reduce the penalty from electricity company. If the BSS reservoir is more than the pre-set value or in the case of critical maximum demand, the battery will discharge accordingly. If it is less than the value set in the reserve, the battery will be charged during low demand by the PV system. In short, this can help consumers save energy by reducing the fines for exceeding the maximum demand, flattening the load profile with the ability to be scaled up for use in all types of buildings [11].

2. WORKING PRINCIPLE

2.1 Block diagram of the mechanism

Fig. 2 shows the modified block diagram of the peak shaving mechanism. The switching mechanism is implemented into the controller instead of using controllable switches. This is one of the methods for reducing the computational time during simulation. The load profile can be placed as part of the load, and as a result of the forecasting mechanism [12], can be linked directly to the model as part of the power generated from the PV system [13]. The algorithm in the controller is used to determine the charge-discharge operation based on the SOC, time, PV availability, and the maximum demand set. The switching mechanism can then be switched between charging, discharging, or remain idle in the given conditions to effectively shave the selected

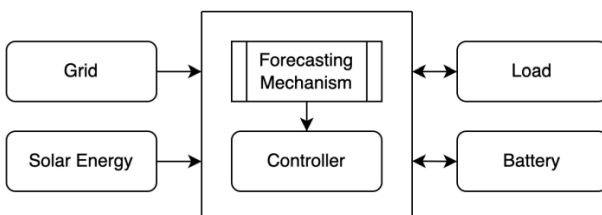


Fig. 2: Proposed block diagram of the simulation model.

Table 1: Summary of the operating system.

Time of day	Condition	Battery	Output
Peak	Does not exceed the limit	Charge	PV to battery and load
	Exceeds the limit set	Discharge	PV and BSS to load
	Not within the SOC range	Idle	PV fully to load
Off-Peak	Less than maximum SOC	Charge	Grid to BSS
	Exceeds maximum SOC	Idle	Grid to load

peaks. Peak selection is performed by adjusting the maximum demand limit. Additional parameters are added to prevent harmonics from damaging the grid.

2.2 Flowchart of the mechanism

The flowchart for the peak shaving mechanism is presented in Fig. 3. First, the load profile along with the forecasted PV results are loaded into the simulation model, forming the basis of the forecasting mechanism. The simulation model is designed to take in the demand of the load profile and power generated from the PV system in a day directly in the form of a spreadsheet. The data in the spreadsheet directly form the output of the load profile and power generated from the PV system in the Simulink model, neglecting any form of data conversion.

The mechanism starts by determining the time of day. During the day at peak periods, the BSS operates based on its SOC. When the SOC is within range, it continues its charge-discharge operation since this indicates that the BSS has sufficient energy to perform its task. When the demand exceeds the limit set, the BSS starts discharging to shave the peak, along with the PV system. The BSS will only be charged by the PV system during the day to minimize the demand and energy consumption from the load. When the SOC exceeds the limit set, the BSS will remain idle and wait for a further change in conditions to prevent overcharging. During off-peak hours, the battery will either remain idle when the SOC reaches the upper limit, or be charged by the grid when it is at less than the maximum SOC. The rate for consumption (cent/kWh) during off-peak hours is lower for some tariffs compared to the rate charged during the day. Thus, utilizing night charging can reduce monthly electricity costs. The operation is summarized in Table 1.

It is recommended that the battery go no lower than 50% and above 80% at the upper limit. If these limits are exceeded, the battery will be subject to rapid degradation and stress [14]. Therefore, a limit is set for the BSS to be in idle mode when out of the SOC range. The range varies based on the tasks and various parameters, but for this simulation, the operable SOC is set to between 50% and 80%. Further studies are required to find the ideal SOC range based on the battery size and usage frequency.

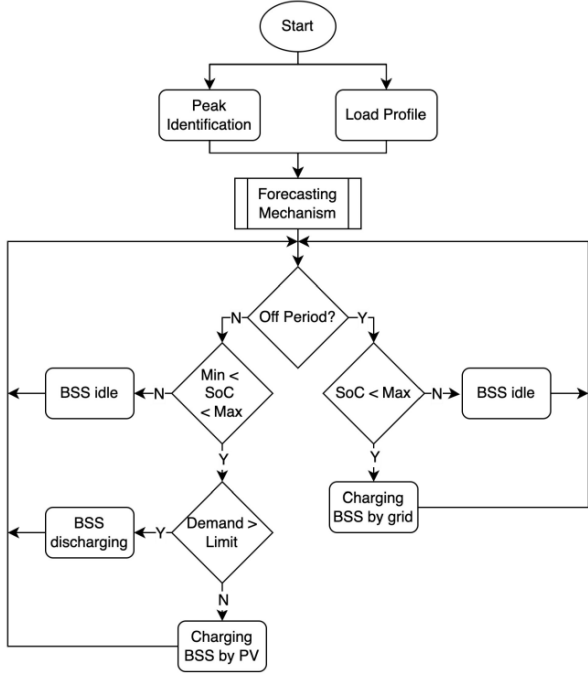


Fig. 3: Flowchart of the overall peak shaving mechanism.

For the mechanism to be adaptive, the load profile needs to be forecasted daily to identify the coming peaks. In the simulation model, the demand limit set triggers the BSS to be charged or discharged. By utilizing load forecasting, the limit can identify the future peaks, enabling the BSS to shave them. To give a better understanding, the load profile used is in real time, while the demand peaks along with the solar peaks are forecasted data.

According to the flowchart in Fig. 3, the load profile and forecasted data are first prepared in the form of a spreadsheet. The model will then determine the time of day. During peak hours, the BSS will be in operation, ready to charge or discharge based on the SOC and demand limit. The BSS will be fully charged by the PV system only during the day. During off-peak hours, the BSS will be charged from the grid until it reaches the maximum SOC. It should be noted that this flowchart only applies to 24-hour data in seconds.

2.3 Sizing the BSS

Sizing of BSS is achieved through HOMER PRO [5]. The BSS size is optimized using the PV size and the load profile while limiting the power supplied from the grid. The method recommended by [10] is used to determine the correct sizing for the battery to maximize revenue. The setting details for the sizing are shown in Tables 2 and 3.

The spike-to-battery ratio indicates whether or not the battery can completely eliminate the spikes. If this ratio is greater than 1, the battery energy capacity is not sufficient for eliminating the spikes. Therefore, it would

Table 2: Report of the PV system produced from the homer pro based on the load profile. the 400kW is used to obtain the optimum BSS sizing.

Generic Flat Plate PV Electrical Summary		
Minimum Output	0	kW
Maximum Output	386	kW
PV Penetration	56.5	%
Hours of Operation	4360	hrs/yr
Levelized Cost	0	RM/kWh
Generic Flat Plate PV Statistic		
Rated Capacity	400	kW
Mean Output	72.1	kW
Mean Output	1730	kWh/d
Capacity Factor	18.0	%
Total Production	631, 423	kWh/yr

Table 3: Report of the battery sizing based on the proposed profile.

Generic 1kWh Li-Ion (ASM) Properties		
Batteries	200	Qty
String Size	20.0	Batteries
Strings in Parallel	10.0	Strings
Bus Voltage	74.0	V
Generic 1kWh Li-Ion (ASM) Result Data		
Average Energy Cost	0	RM/kWh
Energy In	528	kWh/yr
Energy Out	483	kWh/yr
Storage Depletion	3.66	kWh/yr
Losses	48.0	kWh/yr
Annual Throughput	508	kWh/yr
Generic 1kWh Li-Ion (ASM) Statistic		
Autonomy	1.12	hr
Storage Wear Cost	14.4	RM/kWh
Nominal Capacity	204	kWh
Usable Nominal Capacity	123	kWh
Lifetime Throughput	7, 614	kWh
Expected Life	15.0	yr

be advisable for the ratio to be less than 1 at the maximum rated power. The threshold ratio helps to determine the size of the battery. This metric shows the relationship between the load shape and peak demand reduction, changing according to the shape of the load spikes in the form of wide or thin. The higher the threshold ratio, the better the economic benefit.

To obtain the threshold ratio, the spike-to-battery ratio over the months is first calculated.

$$Target = \max_{t \in T} (Load_t) - kW_{Battery} \quad (1)$$

$$Max\ Spike = \max_S \left(\frac{\sum_{t \in S} (Load_t - Target)}{4} \right) \quad (2)$$

$$Spike - To - Battery = \frac{\text{median}_{t \in T} (Max\ Spike_m)}{kWh_{Battery}} \quad (3)$$

T is the time segment t in the billing period, $kWh_{Battery}$ is the rated battery, S is the set of all spikes S_i , $Max\ Spike$ is divided by four to convert power to energy at 15-minute intervals. M is the months of m , and $kWh_{Battery}$ is the energy capacity of the battery.

$$Threshold\ ratio = \frac{Lowest\ Spike - To - Battery}{Max\ rated\ power\ output} \quad (4)$$

$$Revenue = a \times e^{b \times Threshold} + c \quad (5)$$

2.4 The simulation model

To create the model, the components must first be prepared. The components can be found in the library provided by LeSage. Here, the BSS, varying load profile, and PV system are designed using basic Simulink-Simscape components as shown in Fig. 5. To supply power to the grid, a three-phase source is used, paired with a three-phase transformer. Each component is linked to the utility grid, forming the main system of the simulation model. The components are designed in the form of subsystems to provide a cleaner layout and arrangement for the simulation model. The measurement taken from the PV system, BSS, grid, load, and limit allows the algorithm to control the controller, energy calculator, and pricing calculator.

Fig. 6 shows the subcomponents of the PV system. The PV system is modeled using a three-phase dynamic load. The forecasted PV data can be connected straight to this model to generate the desired output in simulation. The results will show a similar output to the forecasted result in the measurement scopes; therefore, no additional changes are needed to convert the datatype to fit the simulation.

A similar approach is applied to create the variable load model presented in Fig. 7. The three-phase dynamic load is subjected to dynamic load control. This allows for easy placement of the load profile in the form of a spreadsheet or MATLAB workspace without the requirement for it to be converted to any datatype. The dynamic load control for this model considers the power factor of the load.

The BSS model presented in Fig. 4 is extracted from the library provided by LeSage (2021) and acts as the BSS for the simulation model. A variable load is used to control the battery current. Various parameters can be tuned with this model, namely the upper and lower limits of the BSS that will determine the charge-discharge operation, the initial SOC, power kW , and its capacity in kWh . Additional options such as efficiency and charging rate can be set as well. The model will be in phasor to quicken the computational time; thus, the power measurement must be converted to phasor.

Fig. 8 shows the controller used to control the overall system. The controller is designed using the Stateflow feature provided in Simulink. The controller is made up of four states, with each respective function executed based on the conditions set.

The first state “disableBSS” acts as an on-off switch. This is used if the BSS is required to be isolated from the main grid for any reason. The second state puts the BSS into the idle mode, meaning no charging or discharging occurs for the BSS. This state occurs during off-peak hours and when the BSS reaches its maximum SOC set. In the third state, the night charging of the BSS is performed by the grid. The BSS is charged by the grid in accordance with the night charging schedule set until the maximum SOC is reached or the night charging schedule is complete. Here, a power limit to charge the BSS by the grid can be set in the Stateflow symbol. In the final state, the daytime operation of the BSS is executed, with the BSS being charged by the PV system and discharged when the demand exceeds the limit set.

Additional conditions are set to allow the BSS to be in idle mode during the operation stage to prevent the grid from being harmed by the occurrence of harmonics. Harmonics in this system are caused by the constant switching between operational modes if the SOC fluctuates between the limits, lowering efficiency and potentially tripping the circuit breakers of the system.

Fig. 9 shows the measurements taken from the PV system, BSS, grid, load, and limit. For each component, specific parameters are obtained for use in the controller, energy calculator, and pricing calculator. The load demand in kW , SOC of the battery, power generated from the PV system, and limit are used as the parameters for the controller. To construct the energy calculator, the load profile and grid power measurements are both integrated with respect to time to obtain the energy in kWh , as presented in Fig. 10. The load in kWh represents the energy consumed by the load prior to the use of alternative sources. The grid in kWh indicates the energy consumed by the load by considering the PV and BSS. The shaved kWh indicates the amount of energy shaved by obtaining the difference between the load and grid. The grid in kWh is then used to develop the price calculator.

Eqs. (6) and (7) are used to calculate the total energy of the components and energy shaved, as well as for constructing the energy calculator and tariff C1 pricing calculator.

$$E = \int_{t_1}^{t_2} P(t) dt \quad (6)$$

$$E_{Shaved} = E_{Load} - E_{Grid} \quad (7)$$

The complete simulation model is displayed in Fig. 13.

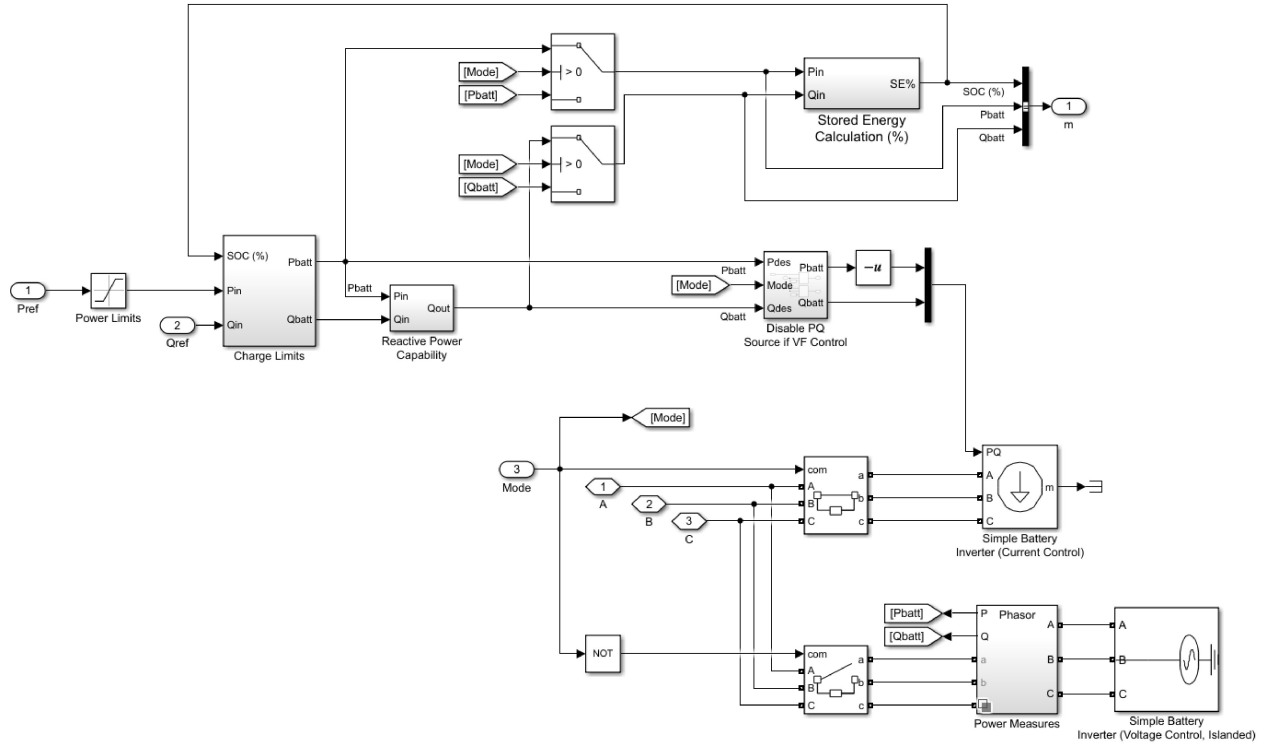


Fig. 4: The BSS model used in this study.

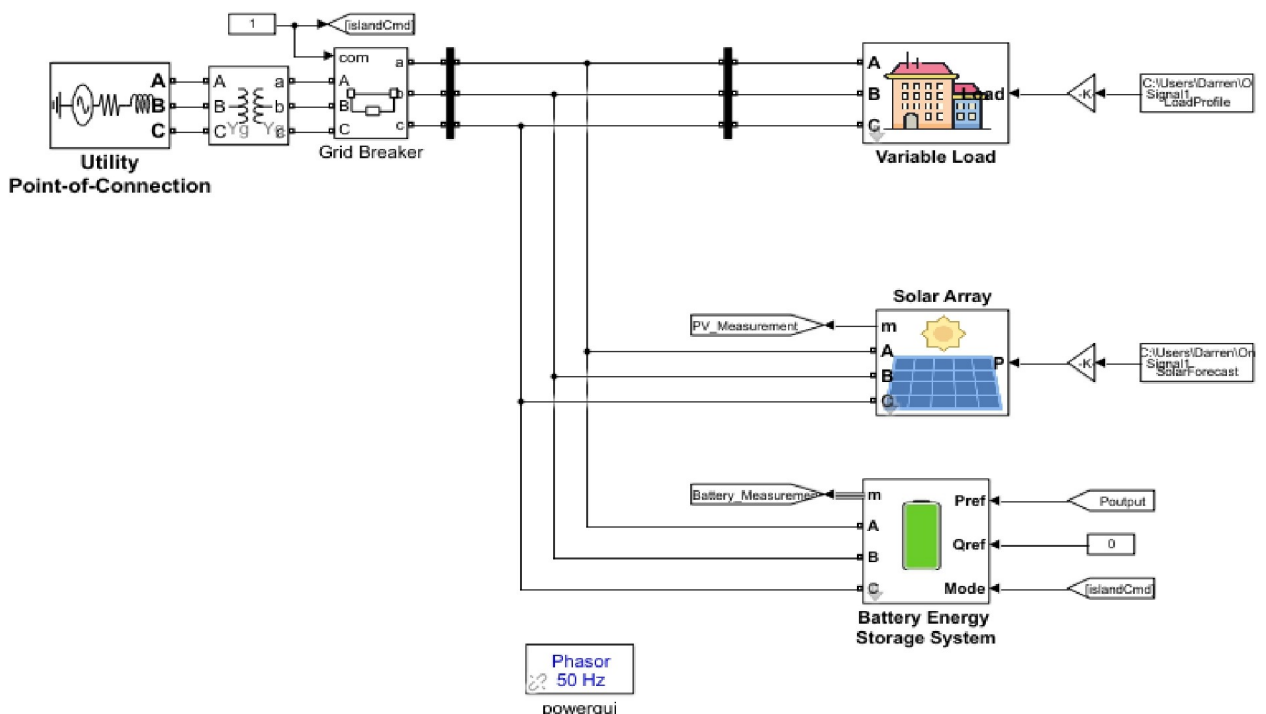


Fig. 5: Main components of the simulation model in SIMULINK.

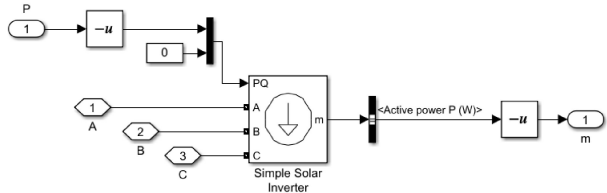


Fig. 6: The PV model constructed using a three-phase dynamic load.

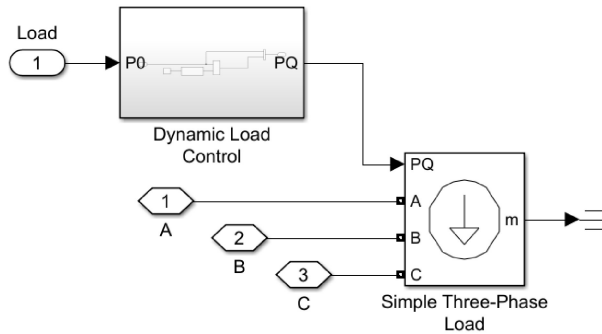


Fig. 7: The variable load model constructed using a three-phase dynamic load.

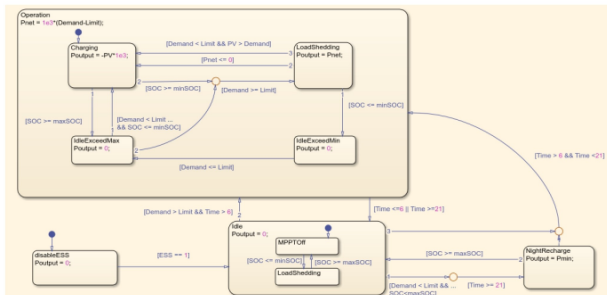


Fig. 8: The algorithm of the controller used for the peak shaving mechanism in Stateflow.

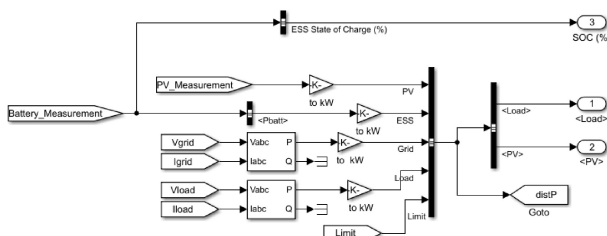


Fig. 9: The measurement of all components.

3. SIMULATION OF PROPOSED MECHANISM

3.1 Generated data with fixed maximum demand

This test utilizes the *signal generator* block to produce the load profile and forecasted PV data for the peak shaving mechanism. The load profile produced by the signal generator block consists of two peaks, exceeding the fixed demand limit set, whereas the forecasted PV data provide power during the day and peaks at noon.

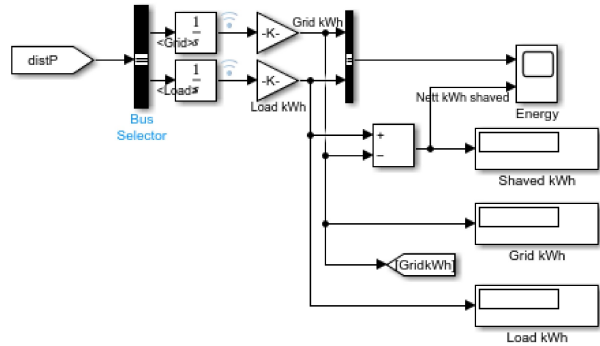


Fig. 10: The energy calculator.

The purpose of the test is to determine whether the designed system can perform as expected.

The *signal generator* blocks are used to produce the load profile and forecasted PV data for this test. The signals generated can be observed in Figs. 11 and 12. Both generated signals are connected to the respective loads and PV blocks to simulate the data in the form of output energy. A fixed constant is added to serve as the fixed demand limit that triggers the battery charge-discharge operation. This is achieved using the *constant* block and setting a value for it. The limit for the SOC of the BSS is set to operate within 50 to 80%. The simulation is left to run with a stop time of 86400 s in phasor mode. The output for the power PV, BSS, grid, load, and limit are recorded to observe and compare the before and after peak shaving results. The grid voltage in Vrms and the SOC of the BSS are also recorded.

Fig. 14 shows the results obtained from the test. The load profile and forecasted PV follow the waveform of the *signal generator* blocks, amplified by their respective multipliers. The demand limit is fixed throughout the simulation. The grid shows the net power received by the load after the peak shaving mechanism is employed. The SOC of the BSS is displayed as the battery reservoir in percentage terms.

Accordingly, the load profile contains three peaks that require shaving. Thus, the peak shaving mechanism is activated three times, since the load demand exceeds the limit. Each time the peak shaving mechanism is activated, the grid power supplying the load is reduced and the power from the BSS increased. This shows that the BSS is discharging to provide power to the load, as can be observed in the graph showing the BSS SOC decreasing from 80 to 50%. Once the load profile is less than the fixed demand limit, the BSS will be charged by the PV system, as indicated by the negative power, until reaching its upper limit of 80%. Night recharging can also be observed at the start of the simulation when the battery increases from 60 to 80%, with the grid power increasing to 30kW to charge the BSS.

This test shows that the peak shaving mechanism is working as expected. The mechanism is able to shave the peak according to the fixed demand limit. The BSS can charge-discharge with no harmonics occurring during

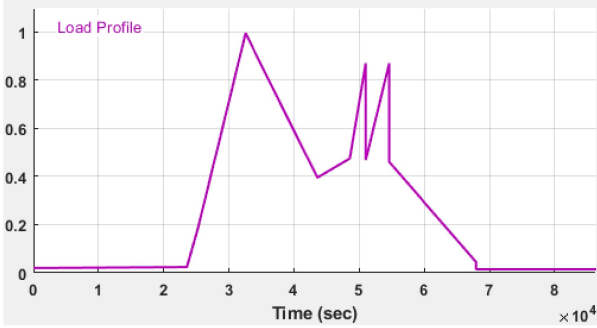


Fig. 11: Generated load profile via the signal generator block.

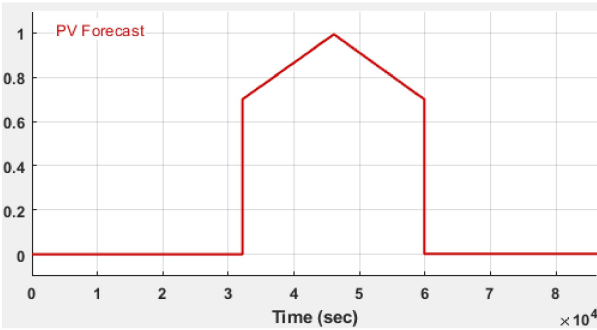


Fig. 12: Generated PV forecast via the signal generator block.

the idle state. This is largely due to the additional conditions set in the controller. The BSS SOC did not exceed the operational limits set either, thus lowering battery degradation and stress. Additionally, the night recharging process follows the schedule set in the controller.

The grid voltage fluctuates according to the load profile after peak shaving. When grid power supplied to the load decreases, so does the grid voltage. Vice versa, with an increase in the grid power supplied to the load, the grid voltage also increases. Since the change in grid voltage is small, it can be said to be constant at 5000 Vrms.

Real-time data is required to further inspect the peak shaving mechanism.

3.2 Real data with fixed maximum demand

Fig. 15 shows the results obtained. The demand limit is fixed to 400kW. Multiple peaks can be observed at the load profile. Each peak exceeding the demand limit is shaved by the energy stored in the BSS. Each time the load does not exceed the limit, the BSS is charged. Throughout this test, the grid power supplied remains below the demand limit set, thereby fulfilling the task of the mechanism, even with the fluctuation in power supply by the PV system. It should also be noted that the size of the BSS is optimized for this setup, since its peak shaves with sufficient energy during the day, and without utilizing the night recharging system from the grid. The BSS can operate within the SOC range set. This

reduces the cost of electricity since grid power is not used for recharging at night.

Using tariff C1, the cost of electricity is revealed to be roughly RM9,500 without considering incentives or taxes, the maximum demand is 269.3kW. These results are presented in Fig. 16. The total energy shaved by this setup is 1865 kWh, demonstrated in Fig. 17.

Discrepancies are likely to occur between the simulated results and the proposed mechanism in a real-life scenario. Some parameters are neglected, such as power loss in the cable or the efficiency of the inverters. A small amount of power may be lost during the conversion or transmission phase when the peak shaving mechanism is triggered. This is not demonstrated in the simulation model. Moreover, the pricing calculator does not consider any incentives or taxes and provides only a rough estimate of the electricity cost in comparing the various techniques for adjusting the peak shaving mechanism to maximize the savings. Lastly, the peak shaving mechanism relies heavily on the PV forecast, and although the forecasted results are 95% accurate, there is still a small possibility of error.

The authors in [6] use F-DL as a basis for testing the effectiveness of the developed algorithm [3]. The same approach is applied to the algorithm in this study. The findings reveal a minor improvement over the use of the developed algorithm when compared with the F-DL method, which is similar to observations reported in the previous work. The main difference is that the authors in [6] utilize generators for peak shaving with their own proposed algorithm rather than the BSS and PV system. This shows that the peak shaving mechanism works, but requires additional optimization to improve its efficiency.

According to the results of all these tests, the method offering the most benefit is the one utilizing the quantized load forecast as the varying demand limit. With the combination of PV forecasting, the demand limit can be optimized to shave the necessary peaks while considering the weather conditions to maximize savings.

During the initial testing, harmonics were present in the system, caused by the constant switching between charging, discharging, and idle state when the SOC fluctuates between the limits. This constant switching harms the system, leading to greater loss in the power system, and a reduction in performance. Additional conditions are therefore set to rectify the position by ensuring that the EMS remains in the correct state, based on the various parameters, thereby preventing harmonics from occurring and harming the system.

Losses are not reflected in this model. To fully study the efficiency of this system, losses from the cable or converters need to be considered. Taking losses from the cable as an example, various parameters such as cable type, area, and length need to be considered to determine the cable losses. This can be rectified by using a three-phase PI section line block on the model. The loss would then be neglected due to insufficient data being available on the cable used for the installation.

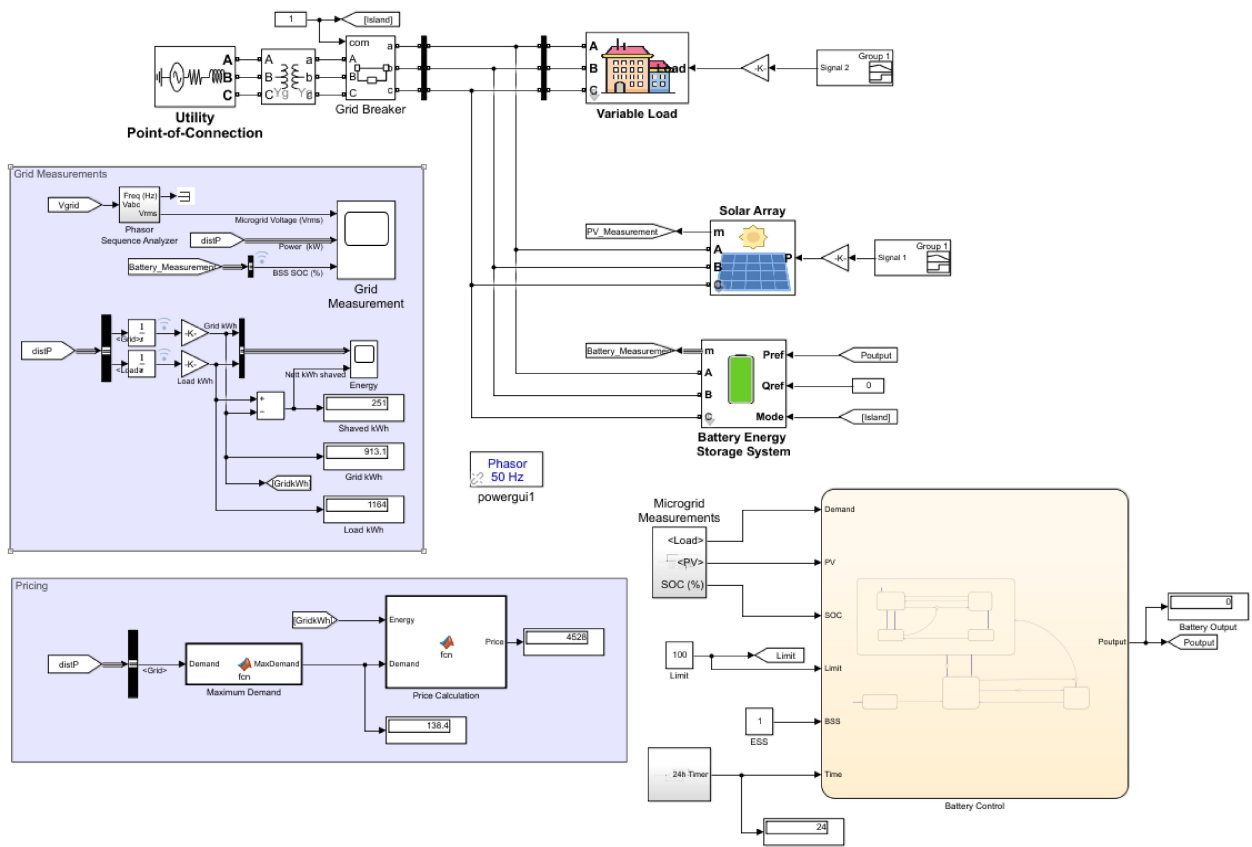


Fig. 13: Full simulation model in Simulink using Signal Builder to analyze the developed algorithm for the controller.

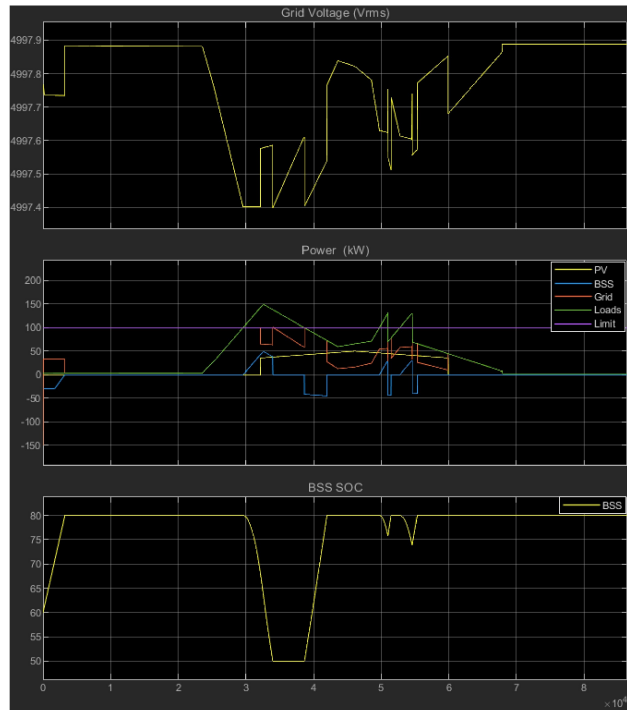


Fig. 14: Output testing using the generated data.

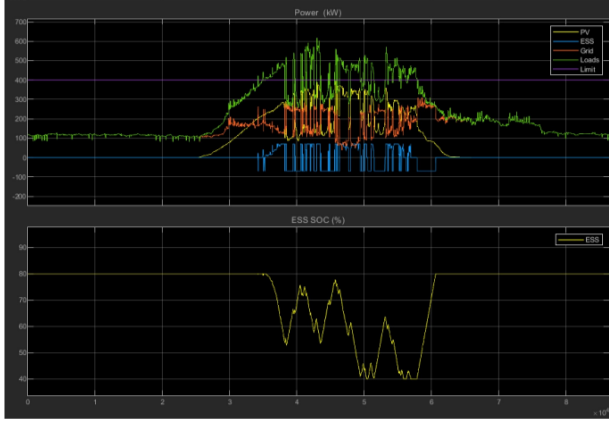


Fig. 15: Output of the simulated result. The output of each component is recorded here.

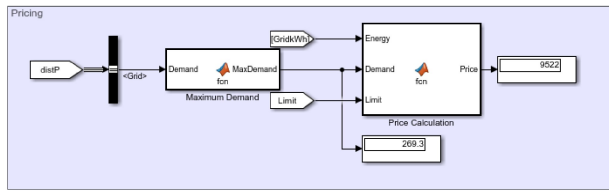


Fig. 16: Estimated price of electricity for the load using the calculator programmed according to the C1 tariff.

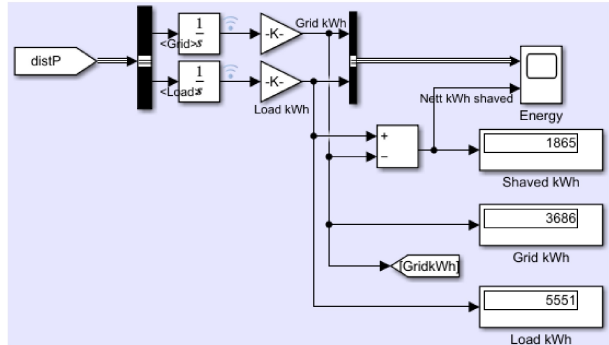


Fig. 17: Energy used before and after peak shaving by the load. The total energy shaved is calculated by finding the difference between the load and grid energy.

4. CONCLUSION

To summarize, the peak shaving mechanism has been successfully developed, implemented, and tested in different conditions and scenarios. The simulation model developed peak shaves using various methods, the most effective being the quantized forecasted load for peak shaving. The adaptive element requires that the forecasted load be used to adjust the ideal peak shaving schedule each day to selectively peak shave and maximize electricity savings. All the objectives stated in this study were met. The first and second objectives were achieved using Stateflow to design the controller for the BSS. The third objective was met by conducting five tests, using varying demand limits, with the quantized

forecasted load demonstrating the best performance. The proposed mechanism has certain limitations, but these can be rectified to further improve its performance and robustness. In future studies, it is recommended that optimization tools be developed for the quantization of the forecasted load as a varying demand limit.

REFERENCES

- [1] M. F. Sulaima, N. Y. Dahlan, Z. M. Yasin, M. M. Rosli, Z. Omar, and M. Y. Hassan, "A review of electricity pricing in peninsular Malaysia: Empirical investigation about the appropriateness of Enhanced Time of Use (ETOU) electricity tariff," *Renewable and Sustainable Energy Reviews*, vol. 110, pp. 348-367, Aug. 2019.
- [2] M. T. Hussain, N. B. Sulaiman, M. S. Hussain, and M. Jabir, "Optimal Management strategies to solve issues of grid having Electric Vehicles (EV): A review," *Journal of Energy Storage*, vol. 33, no. 102114, Jan. 2021.
- [3] D. Groppi, A. Pfeifer, D. A. Garcia, G. Krajačić, and N. Duić, "A review on energy storage and demand side management solutions in smart energy islands," *Renewable and Sustainable Energy Reviews*, vol. 135, no. 110183, Jan. 2021.
- [4] M. Uddin, M. F. Romlie, M. F. Abdullah, S. Abd Halim, and T. C. Kwang, "A review on peak load shaving strategies," *Renewable and Sustainable Energy Reviews*, vol. 82, pp. 3323-3332, Feb. 2018.
- [5] V. Sohoni, S. Gupta, and R. Nema, "Design of wind-PV based hybrid standalone energy systems for three sites in central India," *ECTI Transactions on Electrical Engineering, Electronics, and Communications*, vol. 17, no. 1, pp. 24-34, Feb. 2019.
- [6] M. Uddin, M. Romlie, M. Abdullah, C. Tan, G. Shafiullah, and A. H. A. Bakar, "A novel peak shaving algorithm for islanded microgrid using battery energy storage system," *Energy*, vol. 196, no. 117084, Apr. 2020.
- [7] S. C. Kim, P. Ray, and S. S. Reddy, "Features of smart grid technologies: An overview," *ECTI Transactions on Electrical Engineering, Electronics, and Communications*, vol. 17, no. 2, pp. 169-180, Aug. 2019.
- [8] M. Shamshiri, C. K. Gan, J. Sardi, M. T. Au, and W. H. Tee, "Design of battery storage system for malaysian low voltage distribution network with the presence of residential solar photovoltaic system," *Energies*, vol. 13, no. 18, no. 4887, Jun. 2020.
- [9] S. Thorat and V. N. Kalkhambkar, "Management of a Solar-PV System with Energy Storage," *ECTI Transactions on Electrical Engineering, Electronics, and Communications*, vol. 19, no. 3, pp. 233-245, Oct. 2021.
- [10] M. Fisher, J. Whitacre, and J. Apt, "A Simple Metric for Predicting Revenue from Electric Peak-Shaving and Optimal Battery Sizing," *Energy Technology*, vol. 6, no. 4, pp. 649-657, Apr. 2018.

- [11] K. Ananda-Rao, R. Ali, and S. Tanisella, "Battery energy storage system assessment in a designed battery controller for load leveling and peak shaving applications," *Journal of Renewable and Sustainable Energy*, vol. 9, no. 4, Jul. 2017.
- [12] S. M. Babbar, C. Y. Lau, and K. F. Thang, "Long Term Solar Power Generation Prediction using Adaboost as a Hybrid of Linear and Non-linear Machine Learning Model," *International Journal of Advanced Computer Science and Applications*, vol. 12, no. 11, pp. 536-545, 2021.
- [13] K. B. Adam and H. Miyauchi, "Optimization of a Photovoltaic Hybrid Energy Storage System Using Energy Storage Peak Shaving," *International Review of Electrical Engineering (IREE)*, vol. 14, pp. 8-18, Feb. 2019.
- [14] M. Woody, M. Arbabzadeh, G. M. Lewis, G. A. Keoleian, and A. Stefanopoulou, "Strategies to limit degradation and maximize Li-ion battery service lifetime-Critical review and guidance for stakeholders," *Journal of Energy Storage*, vol. 28, no. 101231, Apr. 2020.